Effect of Polymer Amphiphilicity on Loading of a Therapeutic Enzyme into Protective Filamentous and Spherical Polymer Nanocarriers

Eric A. Simone,*,†,‡,§ Thomas D. Dziubla,‡,|| Francheska Colon-Gonzalez,⊥ Dennis E. Discher,‡,# and Vladimir R. Muzykantov*,‡,§,⊥

Department of Bioengineering, University of Pennsylvania, Philadelphia, Pennsylvania 19104, Institute for Translational Medicine and Therapeutics, University of Pennsylvania, Philadelphia, Pennsylvania 19104, Institute for Environmental Medicine, University of Pennsylvania School of Medicine, Philadelphia, Pennsylvania 19104, Department of Chemical and Materials Engineering, University of Kentucky, Lexington, Kentucky 40506, Department of Pharmacology, University of Pennsylvania School of Medicine, Philadelphia, Pennsylvania 19104, Department of Chemical and Biomolecular Engineering, University of Pennsylvania, Philadelphia, Pennsylvania 19104

Received August 9, 2007

Rapid clearance and proteolysis limit delivery and efficacy of protein therapeutics. Loading into biodegradable *polymer nanocarriers* (PNC) might protect proteins, extending therapeutic duration, but loading can be complicated by protein unfolding and inactivation. We encapsulated active enzymes into methoxy-poly(ethylene glycol-*block*-lactic acid) (mPEG-PLA) PNC with a freeze–thaw double emulsion (*J. Controlled Release* **2005**, *102* (2), 427–439). On the basis of concepts of amphiphile self-assembly, we hypothesized that the copolymer block ratio that controls spontaneous curvature would influence PNC morphology and loading. We examined PNC yield, shape, stability, loading, activity, and protease resistance of the antioxidant enzyme, catalase. PNC transitioned from spherical to filamentous shapes with increasing hydrophobic polymer fraction, consistent with trends for self-assembly of lower MW amphiphiles. Importantly, one diblock copolymer formed filamentous particles loaded with significant levels of protease-resistant enzyme, demonstrating for the first time encapsulation of an active therapeutic enzyme into filamentous carriers. PNC morphology also greatly influenced its degradation, offering a new means of controlled delivery.

1. Introduction

Rapid clearance from the circulation, inactivation by nascent proteases and inhibitors, and a lack of affinity for the desired target sites of action limit the utility of potent but labile therapeutic proteins.[2] Diverse drug delivery systems (e.g., natural lipoproteins, liposomes and polymer nanocarriers) are being widely designed in order to maximize drug efficacy and minimize side effects.[3] For example, polyethylene glycol (PEG), a hydrophilic polymer that enhances aqueous solubility, masks drugs and carriers from host defense systems and prolongs circulation in the bloodstream ("stealth" technology).[4,5] Nanocarriers coated with PEG are already in clinical use for the intravascular delivery of antitumor agents, in the form of stealth liposomes (e.g., Doxil).[6] Comparatively little effort has been invested, however, in nanocarrier mediated delivery of therapeutic proteins, which are complicated because activity requires maintaining the protein's native folded state.

Formulations based on synthetic amphiphilic copolymers that consist of hydrophobic blocks with hydrophilic PEG blocks yield a variety of aggregate shapes, namely micelles, vesicles, and frozen particles, a versatile palette of polymer nanocarriers (PNC) with further diversity in size and degradation patterns.[7–9] Relative to stealth liposomes, PNC based on PEG diblock copolymers have greater durability and can maintain a denser PEG brush and thus potentially a stronger stealth effect.[7] Control over polymer composition as well as molecular weight of the diblocks not only produces PNC of diverse morphology, shape, and size,[10,11] but also provides platforms favorable for drug delivery.[12] Rational design of PNC might also provide an array of carrier types for the optimized delivery of diverse therapeutic proteins that impact treatment of multiple pathologies.

Biodegradable copolymers are understandably key to the delivery of therapeutic enzymes with stealth PNC. Enzyme loading into PNC that are also permeable to the enzyme–substrate, yet impermeable to proteases, could additionally provide activity while protecting the enzyme from premature inactivation.[1] Because loss of enzymatic activity due to unfolding in harsh conditions of PNC formulation has represented a major barrier, we have designed a relatively mild freeze–thaw double emulsion method for the encapsulation of *active* catalase, a large 249 kDa tetrameric enzyme, into PEG-PL(G)A (poly lactic-coglycolic acid) PNC.[1] PLGA is a biodegradable FDA-approved copolymer used for the production of drug delivery systems and sutures. Furthermore, H_2O_2, a reactive oxygen species widely implicated in the pathogenesis of many disease conditions,[2] is freely diffusible through PL(G)A.[1] Our previous study

* Address for correspondence. E-mail: esimone@seas.upenn.edu (E.A.S., polymer nanocarriers); muzykant@mail.med.upenn.edu (V.R.M., enzyme therapeutics). Telephone: 215-898-2449(E.A.S.); 215–898–9823(V.R.M.).
† Department of Bioengineering, University of Pennsylvania.
‡ Institute for Translational Medicine and Therapeutics, University of Pennsylvania.
§ Institute for Environmental Medicine, University of Pennsylvania School of Medicine.
|| Department of Chemical and Materials Engineering, University of Kentucky.
⊥ Department of Pharmacology, University of Pennsylvania School of Medicine.
Department of Chemical and Biomolecular Engineering, University of Pennsylvania.

10.1021/bm700888h CCC: $37.00
Published on Web 11/27/2007

documented that catalase encapsulated within PEG-PL(G)A PNC is protected from proteolysis and decomposes H_2O_2 that diffuses through the PNC shell.[1] In this regard, PNC serve as a nanoreactor without the need for traditional drug release. These previous findings form a basis for the development of durable antioxidant and other detoxifying interventions and motivate systematic studies of macromolecular mechanisms that control the salient features of enzyme-loaded PNC systems.

Amphiphilic diblock copolymers are known to self-assemble into supramolecular structures of diverse morphologies, as controlled by the ratio of constituent hydrophobic and hydrophilic domains.[10,11,13] We hypothesized that for PNC composed of hydrophilic PEG and hydrophobic PLA, the % PLA is a key parameter that governs PNC assembly, geometry, and stability as well as enzyme loading, activity, and subsequent protection against proteolysis.

2. Materials and Methods

2.1. Reagents. All chemicals and reagents were purchased from Sigma-Aldrich (St Louis, MO) and used as received unless otherwise stated. Methoxy poly(ethylene glycol) (mPEG) MW 5000 was purchased from Polysciences (Warrington, PA). The enzymes, bovine liver catalase (242 kDa) and horseradish peroxidase, were purchased from Calbiochem (EMD Biosciences, San Diego, CA). 10-Acetyl-3,7-dihydroxyphenoxazine (Amplex Red) was purchased from Molecular Probes (Eugene, OR). Uranyl acetate (UA) was acquired from Electron Microscopy Sciences (Fort Washington, PA).

2.2. Synthesis of Diblock Copolymers. DL-lactide was recrystallized twice in anhydrous ether before mixing with mPEG in stoichiometric ratios to achieve desired molecular weights. Reactants were heated to 140 °C under nitrogen while stirring for 2 h to remove trace water from samples. The temperature was reduced to 120 °C, and stannous octoate (1 wt %) was added to catalyze the ring opening polymerization (ROP) of lactide with mPEG as the initiator. The polymerization was allowed to continue for 6 h. The diblock copolymer was then dissolved in DCM and twice precipitated in cold diethyl ether. Residual solvent was then removed by first drying via rotary evaporation (Safety Vap 205, Buchi, Switzerland), followed by lyophilization (RCT 60, Jouan, Winchester, VA).

Number average molecular weights ($\overline{M_n}$) of bulk copolymers were determined using proton nuclear magnetic resonance (^{1}H NMR). The weight-average molecular weights ($\overline{M_w}$) and polydispersity indices (PDI) were also determined by gel permeation chromatography (HPLC-GPC), with a binary HPLC pump (1525, Waters, Milford, MA), a refractive index detector (2414, Waters), and three serial 7.8 × 300 mm Styragel columns (Waters) using THF as the mobile phase. Chromatograms were analyzed using Breeze version 3.3 software with polystyrene standards used for calibration.

2.3. Nanoparticle Formation. A freeze–thaw double emulsion–solvent evaporation technique was used as previously outlined.[1] Briefly, mPEG–PLA diblock copolymer is dissolved in DCM at 25 mg/ml. A 1 mg/ml catalase solution and a PVA surfactant solution (2 wt %, 87–89% hydrolyzed, $\overline{M_w}$ = 13000–23000) in 20 mM PBS are prepared. The primary emulsion consists of the organic phase (1 mL polymer–DCM mixture) and the aqueous phase (100 μL catalase solution) homogenized at 15 krpm for 1 min in a dry ice–acetone bath with a 7 mm blade homogenizer (Kinemetica Polytron 3100 with a PDTA3007/2 generator, Brinkmann Instruments, Westbury, NY). The primary emulsion is then added to 5 mL of the PVA surfactant solution and homogenized at 15 krpm for 1 min The resultant mixture is added to 10 mL of PVA solution and stirred overnight to allow removal of the residual solvent. The microparticle fraction is removed by a primary centrifugation at 1000 g for 10 min The nanoparticle fraction is collected by subsequent centrifugation at 20000 g for 30 min. The supernatant is then removed and the PNC pellet is resuspended in PBS and purified again by further centrifugation.

2.4. Enzyme Loading Determination. Protein loading was determined via radioisotope labeling and enzymatic activity. Loading via radiolabeling was determined as described before by formulating PNC with ^{125}I-labeled catalase.[1] Catalase was radiolabeled with Na^{125}I (Perkin-Elmer, Boston, MA) via the Iodogen method (Pierce Biotechnology, Rockford, IL). Unbound ^{125}I was removed from catalase using Biospin 6 columns in accordance with the manufacturer's instructions (Bio-Rad Laboratories, Hercules, CA). Total solution ^{125}I-catalase content was measured before centrifugation, and then radioactivity of the ^{125}I-catalase/PNC-composed pellet after centrifugation was measured. A Wizard 1470 gamma counter (Wallac, Oy, Turku, Finland) was used for radiotracing.

To determine loading via enzymatic activity, a catalase activity assay[14] was used both for the total sample before and after centrifugation. Briefly, 900 μL of 5 mM H_2O_2 in PBS and 100 μL of enzyme-loaded PNC was added to a quartz cuvette. The kinetics of H_2O_2 degradation was then measured with a spectrophotometer at 242 nm (absorbance at this wavelength corresponds to the H_2O_2 concentration; 1 Unit = 23, ΔAbs/ml).

2.5. Catalase Protection Against Proteolysis. Protection against proteolysis was tested as described previously.[1] Briefly, PNC preps loaded with ^{125}I-catalase were incubated with a 0.2 wt % protease (Pronase) solution at 37 °C in a shaker bath set at 60 rpm for 1 h. Samples were removed and centrifuged at 16000*g* for 20 min. Supernatant-containing degraded protein and pellet-containing intact protein encapsulated within PNC were collected and counted.

2.6. In Vitro Degradation of PNC. Solutions of neutral physiologic (pH 7.4) PBS, moderately acidic lysosomal-mimetic (pH 5.0) MES, and strongly acidic (pH 2.5) sodium citrate were prepared. A buffer concentration of 150 mM was selected for these solutions to ensure that the buffering capacity would not be saturated during polymer degradation and lactic acid accumulation. On the basis of the Henderson–Hasselbach equation, complete degradation of $PNC_{65\ kDa}$ polymer would result in a maximum pH change of 0.011. PNC formulations were incubated in these buffer solutions in a shaker bath at 37 °C, shaking at 60 rpm to minimize sedimentation (50-Reciprocating shaker bath, Precision-Jouan, Inc., Winchester, VA). Samples for transmission electron microscopy (TEM), GPC, and lactic acid content assays were taken weekly over the 28-day duration of the study.

2.7. PNC Size Determination. Aliquots of 20 μL (for PNC size measurements) collected at the onset of the study and every 3 days afterward were placed in NMR tubes and diluted with 200 μL of the appropriate pH buffer in triplicate. Size and relative number of PNC, proportional to measured scattering intensity, were determined via dynamic light scattering (DLS, 90Plus particle sizer, Brookhaven Instruments, Holtsville, NY). When we adapt a classical scattering expression for PNC, it is evident that the average intensity of the scattered light is proportional to the actual number of scattering components present in the sample, i.e., $\langle I \rangle \propto N M^2 P(\theta)$, where N is the number of independent particles of size M, and $P(\theta)$ is the sample scattering factor at scattering angle θ.[15,16] While there exist novel methods for counting the precise number of nanoparticles,[17] the relative number as determined by scattering intensity is adequate for this study.

2.8. PNC Concentration Determination. PNC yield was determined via a colorimetric PEG assay based on the PEG-barium iodide complex. Prior to the assay, two solutions have been prepared: solution A, consisting of 2.4 g of barium chloride, 8.0 mL of 6 M HCl, and 32 mL of deionized (DI) water, and solution B, consisting of 800 mg of potassium iodide, 500 mg of iodine, and 40 mL of DI water. A 50 μL aliquot of PNC sample was hydrolyzed by adding 200 μL of 5 M NaOH and incubating overnight at 80 °C. The pH of hydrolyzed PNC samples was then neutralized by addition of 5 M HCl, and 20 μL aliquots were added to a multiwell plate and diluted to a 170 μL total volume with DI water. Subsequently, 40 μL of undiluted solution A and 1/5 diluted solution B were then added to each well. After a 10 min incubation at room temperatu

Table 1. Synthesized Polymer Characterization[a]

target PLA $\overline{M}_n$	PLA $\overline{M}_n$[b]	% PLA	PLA $\overline{M}_n$[c]	PLA $\overline{M}_w$[c]	PDI
1000	791.0	13.7	6032.8	6629.4	1.1
5000	2956.2	37.2	5666.2	6190.2	1.1
8000	6575.5	56.8	3898.9	7253.0	1.4
10000	8482.7	62.9	9974.1	11649.9	1.1
20000	18226.7	78.5	23236.7	36908.2	1.5
25000	21252.7	81.0	21497.8	34530.8	1.5
30000	27091.3	84.4	21859.0	35792.4	1.5
35000	34557.6	87.4	21079.4	39442.7	1.7
65000	64330.2	92.8	19169.4	37650.1	1.8

[a] Number and weight average molecular weights ($\overline{M}_n$ and $\overline{M}_w$, respectively) and polydispersities (PDI, defined as $\overline{M}_w/\overline{M}_n$). Actual % PLA, or wt % PLA, is defined as the ratio of the actual PLA block $\overline{M}_n$ to the entire diblock copolymer $\overline{M}_n$. All diblocks contain a methoxy end-capped 5000 MW mPEG, which served as the initiator for the ring opening polymerization (ROP) of lactide into PLA. [b] Determined by ^{1}H NMR. [c] Determined by GPC.

absorbance of the colored product was measured at 550 nm using the microplate reader.[18] Standard solutions of PEG (5000 MW) were used for calibration.

For 100% PLA PNC, an enzymatic assay based on the detection of lactic acid monomer[1] was used. Samples were hydrolyzed to their monomer state and neutralized as described above. Aliquots were similarly added to a multiwell plate. Then 50 μL of the assay buffer, consisting of 100 μL of 50 mU of lactate oxidase, 100 μL of 10 U ml^{-1} of horseradish peroxidase (HRP), and 50 μL of 10 mM Amplex Red in DMSO were added to each well. Lactate oxidase produces hydrogen peroxide in the presence of lactic acid, and the formed H_2O_2 is decomposed by HRP in the presence of Amplex Red, forming the fluorescent resorufin product. After incubating for 10 min at ambient conditions, the resorufin concentration was determined by UV absorbance at 550 nm on a microplate reader (model 2550-UV, Bio-Rad Laboratories, Hercules, CA). Pure lactic acid solutions were used for calibration.

2.9. PNC Morphology Study. PNC morphology was determined by fluorescence microscopy and transmission electron microscopy (TEM). For fluorescence microscopy, aliquots of PNC were stained with the lipophilic carbocyanine dye, PKH26, via established methods[19] and then imaged with a Nikon confocal microscope equipped with a 60× oil immersion objective. For electron microscopy, 5 μL of each sample were applied to a separate TEM mesh grid (Formvar Film 200 mesh, Electron Microscopy Sciences, Hatfield, PA) and excess was removed before drying. Samples were stained with filtered (0.1 μm filter) 2 wt % uranyl acetate (UA) for 5 min in the dark and then washed with filtered DI water. Grids were dried at ambient conditions for 1 h before they were imaged on a JEOL JEM-100CX TEM.

3. Results

Various PLA molecular weights (MW's) and, consequently, block copolymer MW ratios, were investigated in terms of resultant PNC morphology, enzyme loading, and cargo protection from proteolytic degradation. By controlling reaction feed ratios, ring-opening polymerization (ROP) of lactide with a monomethoxy-capped mPEG initiator yielded mPEG–PLA with PLA block MW's from 800 to 64000 Da (see Table 1) as determined by ^{1}H NMR. The resultant wt % PLA, or "% PLA", defined as the ratio of PLA MW to the total diblock MW, is also shown in Table 1. The polydispersity indices (PDI) of the polymers, determined using GPC, slightly increased with increasing MW, from 1.1 for smaller PLA polymers to 1.8 for the largest ones, as expected for ROP products. MW of the PEG block was kept constant at 5000 Da. The formulation scheme utilized throughout these studies for nanocarrier synthesis and protein encapsulation and the resultant morphology is illustrated in Figure 1A.

3.1. PLA Content in PLA–PEG Diblock Controls PNC Yield and Morphology. PLA MW influenced yield and morphology of PNC formulated by the freeze thaw emulsification process (Figure 1B,C and Figure 2). Final PNC concentration in the nanoscale fraction of the particles was determined by quantitative analysis of PEG or lactic acid content. For the 100% PLA PNC, polymer mass was determined solely by measuring lactic acid content. For the diblock coplymers, either assay could be used to measure total polymer mass in the PNC due to the equimolar ratio of the PEG block to the PLA block. For example, using a PEG assay, the total mass of a diblock made with 5000 Da PEG would be

$$\text{diblock MW} = \left\{\frac{x\ \text{(g, PEG)}}{5000\ \text{(g/mol, PEG)}} \times [y\ \text{(g/mol, PLA)}]\right\} + [x\ \text{(g, PEG)}]$$

We found that diblocks containing 60–100% PLA provided a significant yield (Figure 1B) of nanoscale particles with mean diameters ranging from 200 to 600 nm (Figure 1C). A peak in yield and in effective diameter was also seen at ~80–90% PLA.

PLA MW determined PNC geometry in the range of 63–93% PLA content. An increase in hydrophobic PLA fraction above 80% resulted in an abrupt shift from spherical geometry to filamentous structures, evident from fluorescence microscopy (Figure 1C, inset) and TEM (Figure 2). The asymmetric morphology of PNC formed at >80% PLA complicates simple interpretation of DLS measurements (Figure 1C) because the usual Stokes–Einstein equation assumes a spherical hydrodynamic radius. Therefore, size of filamentous PNC was estimated by microscopy. Fluorescence microscopy revealed that PNC with filamentous morphology are flexible in solution, similar to other PEG-diblock based filamentous micelles;[19,20] and TEM of dried PNC shows the assemblies are not only filamentous but also sufficiently robust to withstand drying.

3.2. PLA Content in PLA–PEG Copolymer Modulates PNC Loading and Activity of Loaded Enzymes. To circulate in the bloodstream without mechanical retention in capillaries, spherical-PNC should be submicrometer in diameter. The homogenization in the double emulsion formulation produces PNC of desired size (200–500 nm) yet also reduces enzyme activity and decreases loading of the enzyme drug. The freeze–thaw cycle aids synthesis of enzyme-loaded PNC by both enhancing the amount of loaded enzyme and protecting it from inactivation.[1] Here we tested how loading and resultant activity of the catalase depend on the content of hydrophobic PLA in the PLA–PEG copolymer.

We monitored PNC loading, defined here as the percent of catalase added in the primary emulsion that is entrapped in the *nano* fraction of formulated particles, via radioisotope tracing of ^{125}I-labeled catalase. The enzyme mass loaded in the microsphere population was excluded from this study, as this regime is not useful for the intended drug delivery application of this technology platform. Catalase loading showed a minor peak at 80% PLA and a major peak at 93% PLA. The lowest loading occurred at the extremes of 0 and 100% PLA, respectively.

The highest catalase loading, 46.9%, was observed with 93% PLA (Figure 3A). This result may represent both encapsulation and surface adsorption due to the enhanced hydrophobic nature of the dominant PLA block. Loading of

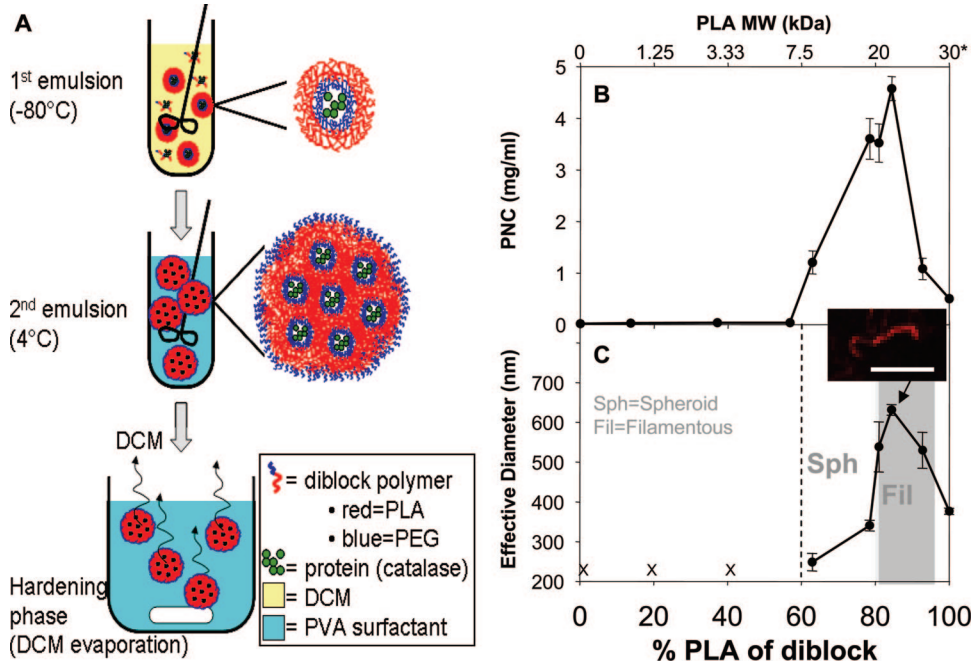

Figure 1. PNC yield and effective size depend on the PLA block MW. Schematic of freeze–thaw emulsion formulated PNC (a). Mass yield of PNC was determined by either PEG or PLA content and all particle preps were resuspended in 1 mL PBS (b). Sizing was determined by DLS (c). "Sph" indicates the spheroid PNC regime, while "Fil" notes the filamentous PNC range. Shades of gray denote PLA percent providing formulation of spherical (white), filamentous (gray), and mixed (light grey) geometries of PNC. Inset shows confocal fluorescent microscopy image of filamentous 84% PLA PNC. Staining was with the lipophilic carbocyanine dye, PKH26 intercalated into the PNC polymer. Scale bar is 5 μm. Data are shown as mean value ± standard deviation.

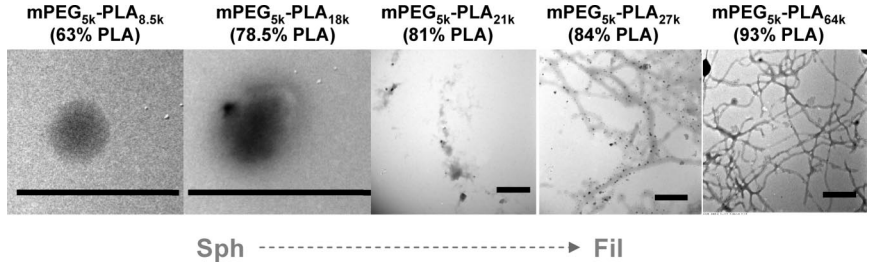

Figure 2. Amphiphilicity of diblock PEG-PLA copolymer controls PNC morphology. Morphologic images are obtained by TEM with uranyl acetate staining. A transition from spherical (60–79% PLA) to mixed populations (80–81% PLA) to filamentous structures (>81–95% PLA) is seen with increasing PLA content. Scale bar is 500 nm.

the sub-60% PLA polymers was negligible (Figure 3A) because PNC did not readily form in this range (Figure 1B). When the PLA content was between 60 and 79% PLA, ≤500 nm spherical PNC were formed with an enzyme loading of 10%, similar to that reported in our previous study on loading catalase into PEG-PL(G)A PNC.[1] When the PLA content was increased over 81%, homogeneous filamentous PNC were formed (Figure 2) with an enzyme loading of 7.2% (for 84% PLA), a loading value similar to that of the spherical PNC.

Important for function, the level of enzyme inactivation during encapsulation also varied as a function of PLA content. Activity loss was the lowest (34.1 ± 10.2% to 41.8 ± 3.6%) between 63% and 84% PLA (Figure 3B). Compositions with PLA MW from 20 to 50% PLA, where there was a negligible PNC yield, caused profound enzyme inactivation (up to 90.9 ± 1.2% activity loss, data not shown), possibly due to the enhanced surfactant nature of the polymers that could affect the protein tertiary structure. Similarly, 89.1 ± 6.8% inactivation was observed when the highly hydrophobic 93% PLA polymer was utilized.

Therefore, PLA MW in the diblock regulated catalase loading (Figure 3A) and resultant activity of the loaded enzyme (Figure 3B). To normalize activity per loading, we defined percent of loaded activity as:

$$\%\ \text{loading} = \left(\frac{\text{activity recovered in PNC}}{\text{added activity}}\right) \times (\%\ \text{activity recovered})$$

where % activity recovered factors in activity lost in the homogenization/formulation process. To the best of our knowledge, this method of loaded-catalase quantification has not been reported before, and it provides a more therapeutically relevant measure of enzyme loading compared to protein mass loading. The analysis shows that the percent of loaded activity was relatively high (approximately 5.2 ± 0.8 to 8.2 ± 2.9%) in the optimal range of 63–84% PLA polymers (Figure 3C).

3.3. Protection of Loaded Enzyme Against External Proteolysis. In the next series of experiments, we tested whether PLA content controls the extent of protection of PNC-catalase against external proteolysis. First, we determined the kinetics of proteolytic inactivation of catalase loaded into 78% PLA PNC (Figure 4A). Free catalase was completely inactivated after incubation for 1 h with the wide-spectrum protease, Pronase, and thus this time is sufficient to test protection of PNC

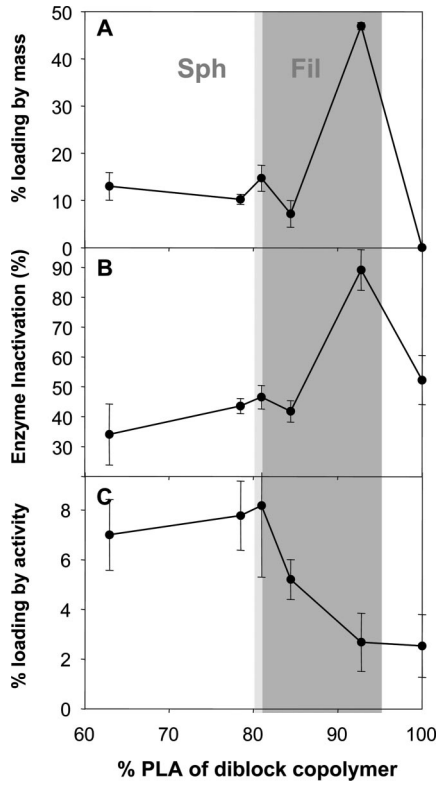

Figure 3. Amphiphilicity of diblock PEG–PLA copolymer controls PNC loading of catalase. Loading by mass is defined as protein mass in PNC divided by the total amount added to the particle prep during the freeze–thaw modified double emulsion formulation (a). Extent of formulation induced enzyme inactivation (b). Enzymatic activity of catalase lost during the formulation homogenizations based on kinetics of H_2O_2 degradation. Percent of activity of total protein mass added is shown. Greatest enzyme protection from formulation occurs between 63 and 84% PLA. Loading of catalase into mPEG–PLA PNC based on enzymatic activity (c). MW region with % PLA < 60% was omitted due to negligible PNC content by polymer mass.

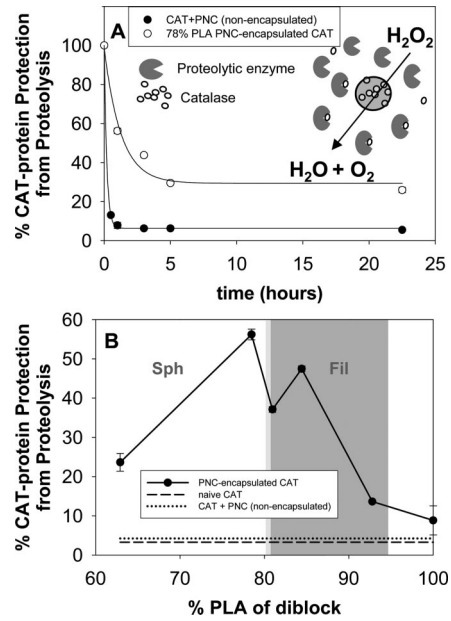

Figure 4. PNC protect catalase (CAT) from proteolytic degradation by Pronase. (a) Activity of free catalase is practically eradicated after 1 h of incubation with pronase. Activity of PNC-loaded catalase decreases by ~70% after 5 h of incubation and stabilizes afterward. Inset illustrates the concept of a PNC "protective cage", which is impermeable to proteases yet freely permeable to the encapsulated enzyme–substrate, H_2O_2. (b) Diverse % PLA PNC loaded with ^{125}I-catalase were incubated with pronase for 1 h, and degraded protein was separated from protected/encapsulated protein by centrifugation. This measure has been shown to correlate linearly with preservation of enzymatic activity.[1]

encapsulated catalase against proteolysis. In this assay, formulations with a low PLA fraction (<60%) provided no measurable protection of catalase (not shown), presumably due to a lack of PNC formation (see Figure 1B). The marginal protection observed at 100% PLA PNC is indicative of primarily surface adsorbed catalase, with no appreciable encapsulation to provide a physical barrier between catalase and a protease. This observation agrees with the proposed mechanism of encapsulation outlined in Figure 1A that requires a well defined amphiphile, which 100% PLA is not.

Loading of catalase into PNC produced with 63–84% PLA copolymer, afforded significant protection against proteolysis (Figure 4B). Loading catalase into PNC produced with 93% PLA copolymer provided little protection (13.6 ± 0.3%), consistent with the hypothesis that the major fraction of the enzyme is surface-adsorbed in this rather hydrophobic filamentous PNC species. However, loading of catalase into either spherical or filamentous PNC, formed at 78% and 84% PLA, respectively, correspondingly provided 56.2 ± 1.4% and 47.5 ± 0.7% protection against proteolysis. Adding unloaded PNC to free catalase provided no protection against proteolysis (Figure 4B, dashed lines), indicating that catalase adsorption on the PNC surface does not provide a secondary protective effect.

3.4. PLA Content, pH of the Medium, and PNC Geometry Modulate PNC Degradation. To characterize copolymer PLA content control of PNC stability at physiologically relevant pH levels, degradation studies were performed at pH 7.4, 5.0, and 2.5, corresponding to normal blood plasma, lysosomal, and stomach pH, respectively. DLS analysis of spherical PNC stability revealed a detectable decrease in the scattering intensity that can be directly correlated with the number of PNC in solution (Figure 5A). There was only a marginal change in diameter of these spherical PNC over time, regardless of pH (Figure 5B). This result likely reflects pH-modulated PNC degradation via bulk erosion rather than surface erosion. Thus, PNC with lower PLA MW (~80% PLA) decreased in number more rapidly with decreasing pH: the number of 80% PLA PNC dropped by ~35% at neutral pH, while at pH 2.5, the number of PNC decreased ~45% with a faster initial drop within the first week. Degradation at pH 5.0 was not significantly different than that at neutral pH (data not shown). Supporting Information Figure 1 shows initial and final effective PNC diameters.

DLS analysis of filamentous PNC is complicated by their geometry and dynamic conformations in solutions. Thus, the effective size of filamentous PNC represents a complex function of their length, flexibility, and coiling. Nevertheless, DLS measurements showed little change in either effective size or concentration of filamentous PNC formed at high PLA content (87% PLA) when incubated at neutral pH over a month (Figure 5C,D, black circles). Importantly, electron microscopy confirmed this result (Figure 6, row 1). In contrast, DLS analysis revealed a notable decrease in effective size of filamentous PNC at acidic pH, which correlated with an increase in the scattering intensity. This increased scattering implies an increased concentration of particulate matter, likely reflecting fragmentation of filamentous PNC (Figure 5C,D, white circles). Again, this DLS result has been confirmed by electron microscopy, which showed a gradual fractionation of filamentous PNC into shorter and eventually

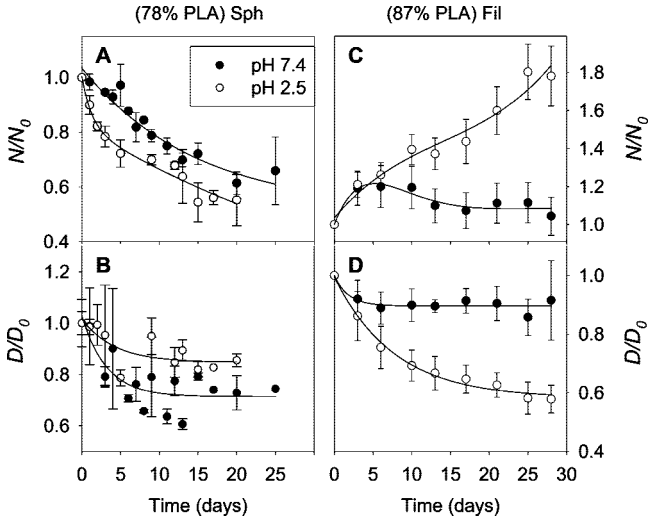

Figure 5. Degradation of spherical and filamentous PNC. Degradation of spherical (78% PLA) PNC by DLS (a,b). A bulk erosion phenomenon is evident from a decrease in the total number of PNC (a) accompanied by a relatively constant measure in effective diameter (b). Degradation of filamentous PNC by DLS (c,d). Change in diameter (d) of filamentous PNC (87% PLA) is heightened at pH 2.5, while little change is seen at either neutral or pH 5.0 (data not shown). Effective diameters correlate with hydrodynamic volume occupied by filamentous PNC, which are coiled in solution, as verified by fluorescence microscopy. Concomitant with a decrease in diameter was an increase in number of filamentous PNC (c). Similar trends were observed with higher MW (93% PLA) filamentous PNC.

spherical structures (Figure 6, row 2). This degradation phenomenon was typical of multiple formulations of filamentous PNC with even higher PLA content (Supporting Information Figure 2).

4. Discussion

Despite the specificity of therapeutic enzymes, medical utility is often limited by inadequate delivery and insufficient stability in the body. Catalase is a naturally occurring antioxidant enzyme that can in principle be used for the treatment of vascular oxidative stress involved in the pathogenesis of many disease conditions.[2] However, catalase and other antioxidant enzymes (e.g., superoxide dismutase) have no practical medical utility due to inadequate delivery to therapeutic sites, especially the endothelial cells lining the luminal surface of blood vessels. Conjugation of enzymes to targeting antibodies improves delivery and effects of antioxidant enzymes in diverse animal models,[21,22] and yet therapeutic duration is limited to a few hours by catalase proteolysis at the target site.[23]

Loading and protection can in principle address the above issues, but maintaining folded and active protein is a general problem and catalase is such a large protein that the challenge is compounded. Our recent studies indicated that encapsulation of catalase into PNC formulated from copolymers combining PEG with more hydrophobic PLA and PLGA blocks may help overcome this problem.[1] We found that addition of a freeze–thaw cycle during the primary emulsion enhances catalase loading into PNC and reduces its formulation-induced inactivation.[1] The primary hypothesis of the present study is that polymer MW and amphiphilicity play a crucial role in the freeze–thaw synthesis of PNC. With constant PEG content, the MW of the PLA block in the diblock copolymer determines the overall amphiphilicity. Thus we tested our hypothesis using PNC composed of a series of diblocks combining a 5000 MW PEG block with PLA blocks of diverse molecular sizes. Of note, these PNC are not typical self-assembled particles formed from solvent-free amphiphiles that have been rehydrated with water, as studied elsewhere.[7] Rather, a more complex structure is likely the case with the present PNC that result from this unique freeze–thaw double emulsion formulation (Figure 1A, blown up PNC cross section).

On the basis of PNC yield and enzyme loading data, copolymers containing 63–84% PLA have sufficient amphiphilicity for formulation of PNC with effective diameters on the order of 500 nm or less, and significant catalase activity that is markedly protected against external proteolysis. PNC in the sub-500 nm range are readily internalized when targeted to appropriate cell surface receptors[23] and thus are plausible candidates for intracellular delivery. Lower PLA content provided no significant PNC yield, whereas catalase inactivation was more profound in more hydrophobic polymers (93% and 100% PLA). The enhanced hydrophobicity of these PNC translates into stronger protein–surface interactions and adsorption that may interfere with the enzyme's activity.[24]

Double emulsion formulations typically produce PNC with both encapsulated and surface adsorbed protein loads. Polymer amphiphilicity appears to control this ratio. Surface adsorbed protein is not protected against proteolysis, as appears to be the case for less amphiphilic, and thus more hydrophobic, 93% PLA PNC. However, filamentous 84% PLA PNC provided protection of encapsulated catalase comparable to that of spherical 78% PLA PNC. This notion of surface adsorption versus encapsulation coincides with the observed enzyme protection from proteolysis for the spherical PNC observed in the 80% PLA range, as has been proven with this system for a similar PEG PNC that was ~80% PL(G)A.[1] It is unlikely that degradation of the polymer itself would contribute to enzyme inactivation. There is no detectable change in either polymer MW by GPC (data not shown) or PNC number over the course of 1 day, the time frame within which catalase activity studies were performed. Further, cross-sectional diameters of 93% PLA filamentous PNC are much smaller than those observed for 84% PLA filamentous PNC (35.4 ± 5.3 nm vs 68.3 ± 7.3 nm, respectively). From a geometric standpoint, the 93% PLA filamentous PNC possessed only 26% of the internal volume per unit length afforded to the 84% filamentous PNC, suggesting that the degree of encapsulation may be dependent upon filament diameter. In other words, the ratio of encapsulated to surface-adsorbed catalase is expected to be lower in 93%, relative to 84%, PLA filamentous PNC, explaining the loss of protease resistance observed in the former formulation.

The PLA MW also controlled shape and degradation of the formed PNC. In the case of spherical PNC, a decrease in PNC number with stable mean diameter is characteristic of bulk erosion and homogeneous degradation of particles: the nominal diameter remains stable until the PNC polymer erodes throughout to a burst point, diminishing the net number of PNC. This coincides with degradation properties observed with polyester PLA and PLGA nanostructures.[25,26] Lowering the pH and polymer MW accelerates the PNC degradation, most likely due to accelerated polymer hydrolysis.

Conversely, the gradual decrease in effective diameter and corresponding increase in number of particles (Figure 5C,D), unexpected for homogeneously degrading nanoscale polyester structures, are suggestive of an alternative mechanism of degradation of filamentous PNC. It would seem that filamentous PNC fragment into shorter filaments and eventually spheres. Thus, this form of degradation may serve as a depot of spheric

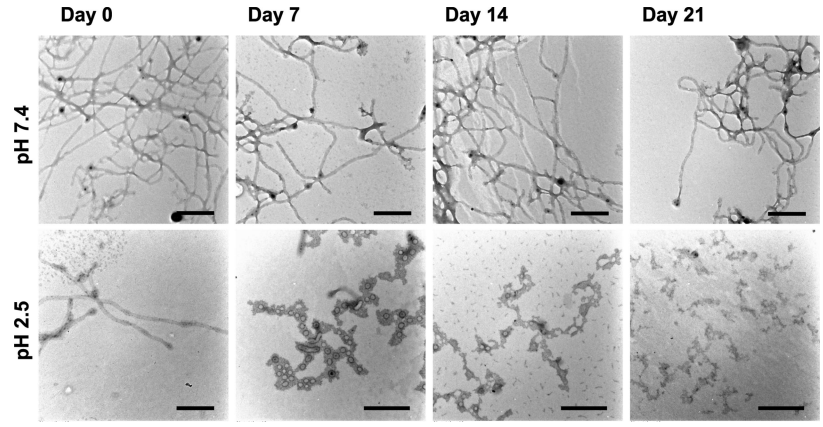

Figure 6. pH influenced degradation of filamentous PNC. Morphology changes of (87% PLA) filamentous PNC by TEM over 1 month degradation in neutral and acidic pH. Filamentous PNC show higher sensitivity at pH 2.5 (row 2), while no morphologic change is evident at neutral pH (row 1). Similar trends for filamentous PNC composed of PEG copolymer with higher PLA MW were observed (see Supporting Information Figure 1). Scale bar is 500 nm.

more diffusible carriers. Similar to spherical PNC, lowering the pH and polymer MW accelerated degradation of the filamentous PNC (Supporting Information Figure 2). This raises an interesting point regarding DLS analysis of nonspherical particles. Light scattering is proportional to both the particle area and the number of particles. As the filamentous structures fragment and become spherical, the diffusion rate increases (resulting in a smaller hydrodynamic radius) but the average cross-sectional area of the light path increases, leading to an increase in scattering. Therefore, the obtained data reflect an increase in the number of particles. In an additional study, we found that disruption of filamentous PNC by ultrasound led to increased scattering intensity that, consistent with our analysis proposed above, reflected an increased number of PNC fragments.

This study for the first time demonstrated simultaneous encapsulation and protection of an active enzyme within filamentous PNC. Recent studies demonstrate that nonspherical carriers may indeed have utility in drug delivery. For instance, nonspherical, oblong particles can be phagocytosed,[27] and many are interested in using nanotube structures for controlled delivery.[28] The unique filamentous morphology offers several potentially advantageous features. For instance, the relatively extensive length translates into a high potential volume for drug cargo loading while the small cross section retains the carrier's *nano* status.[29] This is important, especially in light of new studies where such filamentous nanostructures have shown the potential for unprecedented extended circulation (likely due to alignment with flow), allowing a novel extended release depot delivery system.[30,31]

5. Conclusion

The goal of this study was to determine the importance of polymer amphiphilicity in enzyme loading and cargo stability. When this characteristic is pushed to extremes, enzyme encapsulation suffers. Interestingly, through control of MW composition, this formulation system is capable of producing filamentous carriers containing enzyme cargo that is protected from proteolysis. Ultimately, balancing of amphiphilic character with loading, protection, and degradation resulted in a nanocarrier well suited for the prolonged delivery of enzymes.

Acknowledgement.. This work was supported by grants from the National Institutes of Health (NIH nos. HL007954, HL073940-01-A1, and PO1-HL079063). We thank Tony Lowman and Meredith Hans of Drexel University for their assistance with NMR spectra of our samples and Yan Geng of the University of Georgia for her assistance with GPC characterization.

Supporting Information Available. Specific diameters of degrading spherical nanocarriers as well as electron micrographs of 93% PLA filamentous PNC degradation over the course of a month. This material is available free of charge via the Internet at http://pubs.acs.org.

References and Notes

(1) Dziubla, T. D.; Karim, A.; Muzykantov, V. R. Polymer nanocarriers protecting active enzyme cargo against proteolysis. *J. Controlled Release* **2005**, *102* (2), 427–439.
(2) Muzykantov, V. R. Targeting of superoxide dismutase and catalase to vascular endothelium. *J. Controlled Release* **2001**, *71*, 1–21.
(3) Langer, R. Drug delivery and targeting. *Nature* **1998**, *392* (6679 Suppl), 5–10.
(4) Moghimi, S. M.; Szebeni, J. Stealth liposomes and long circulating nanoparticles: critical issues in pharmacokinetics, opsonization, and protein-binding properties. *Prog. Lipid Res.* **2003**, *42* (6), 463–478.
(5) Roux, E.; Lafleur, M.; Lataste, E.; Moreau, P.; Leroux, J. C. On the Characterization of pH-sensitive Liposome/Polymer Complexes. *Biomacromolecules* **2003**, *4* (2), 240–248.
(6) Lasic, D. D. Product review: doxorubicin in sterically stabilized liposomes. *Nature* **1996**, *380* (6574), 561.
(7) Discher, D. E.; Eisenberg, A. Polymer vesicles. *Science* **2002**, *297* (5583), 967–973.
(8) Zhang, J.; Wang, L. Q.; Wang, H.; Tu, K. Micellization Phenomena of Amphiphilic Block Copolymers Based on Methoxy Poly(ethylene glycol) and Either Crystalline or Amorphous Poly(caprolactone-*b*-lactide). *Biomacromolecules* **2006**, *7* (9), 2492–2500.
(9) Vinogradov, S. V.; Bronich, T. K.; Kabanov, A. V. Self-assembly of polyamine-poly(ethylene glycol) copolymers with phosphorothioate oligonucleotides. *Bioconjugate Chem.* **1998**, *9* (6), 805–812.
(10) Ravenelle, F.; Marchessault, R. H. Self-Assembly of poly([*R*]-3-hydroxybutyric acid)-*block*-poly(ethylene glycol) diblock copolymers. *Biomacromolecules* **2003**, *4* (3), 856–858.
(11) Zhang, L.; Eisenberg, A. Multiple morphologies of "crew-cut" aggregates of polystyrene-*b*-poly(acrylic acid) block copolymers. *Science* **1995**, *268* (5218), 1728–1731.
(12) Alakhov, V. Y.; Kabanov, A. V. Block copolymeric biotransport carriers as versatile vehicles for drug delivery. *Expert Opin. Invest. Drugs* **1998**, *7* (9), 1453–1473.
(13) Israelachvili, J. N.; Mitchell, D. J.; Ninham, B. W. Theory of self-assembly of lipid bilayers and vesicles. *Biochim. Biophys. Acta* **1977**, *470* (2), 185–201.
(14) Shuvaev, V. V.; Dziubla, T.; Wiewrodt, R.; Muzykantov, V. R. Streptavidin–biotin crosslinking of therapeutic enzymes with carrier antibodies: nanoconjugates for protection against endothelial oxidative stress. *Methods Mol. Biol.* **2004**, *283*, 3–19.

(15) Brown, J. C.; Pusey, P. N.; Dietz, R. Photon correlation study of polydisperse samples of polystyrene in cyclohexane. *J. Chem. Phys.* **1975**, *62* (3), 1136–1144.

(16) Tanford, C. *Physical Chemistry of Macromolecules*; Wiley: New York, 1961; p 710.

(17) Epstein, H.; Afergan, E.; Moise, T.; Richter, Y.; Rudich, Y.; Golomb, G. Number-concentration of nanoparticles in liposomal and polymeric multiparticulate preparations: empirical and calculation methods. *Biomaterials* **2006**, *27* (4), 651–659.

(18) Sims, G. E.; Snape, T. J. A method for the estimation of polyethylene glycol in plasma protein fractions. *Anal. Biochem.* **1980**, *107* (1), 60–63.

(19) Dalhaimer, P.; Bates, F. S.; Discher, D. E. Single-molecule visualization of stable, stiffness-tunable, flow-conforming worm micelles. *Macromolecules* **2003**, *36* (18), 6873–6877.

(20) Dalhaimer, P.; Bermudez, H.; Discher, D. E. Biopolymer mimicry with polymeric wormlike micelles: molecular weight scaled flexibility, locked-in curvature, and coexisting microphases. *J. Polym. Sci., Part B: Polym. Phys.* **2004**, *42* (1), 168–176.

(21) Christofidou-Solomidou, M.; Scherpereel, A.; Wiewrodt, R.; Ng, K.; Sweitzer, T.; Arguiri, E.; Shuvaev, V.; Solomides, C. C.; Albelda, S. M.; Muzykantov, V. R. PECAM-directed delivery of catalase to endothelium protects against pulmonary vascular oxidative stress. *Am. J. Physiol. Lung Cell Mol. Physiol.* **2003**, *285* (2), L283–L292.

(22) Kozower, B. D.; Christofidou-Solomidou, M.; Sweitzer, T. D.; Muro, S.; Buerk, D. G.; Solomides, C. C.; Albelda, S. M.; Patterson, G. A.; Muzykantov, V. R. Immunotargeting of catalase to the pulmonary endothelium alleviates oxidative stress and reduces acute lung transplantation injury. *Nat. Biotechnol.* **2003**, *21* (4), 392–398.

(23) Muro, S.; Cui, X.; Gajewski, C.; Murciano, J. C.; Muzykantov, V. R.; Koval, M. Slow intracellular trafficking of catalase nanoparticles targeted to ICAM-1 protects endothelial cells from oxidative stress. *Am. J. Physiol. Cell Physiol.* **2003**, *285* (5), C1339–C1347.

(24) Shuvaev, V. V.; Christofidou-Solomidou, M.; Scherpereel, A.; Simone, E.; Arguiri, E.; Tliba, S.; Pick, J.; Kennel, S.; Albelda, S. M.; Muzykantov, V. R. Factors modulating the delivery and effect of enzymatic cargo conjugated with antibodies targeted to the pulmonary endothelium. *J. Controlled Release* **2007**, *118* (2), 235–244.

(25) von Burkersroda, F.; Schedl, L.; Gopferich, A. Why degradable polymers undergo surface erosion or bulk erosion. *Biomaterials* **2002**, *23* (21), 4221–4231.

(26) Gopferich, A. Polymer bulk erosion. *Macromolecules* **1997**, *30* (9), 2598–2604.

(27) Champion, J. A.; Mitragotri, S. Role of target geometry in phagocytosis. *Proc. Natl. Acad. Sci. U.S.A.* **2006**, *103* (13), 4930–4934.

(28) Son, S. J.; Bai, X.; Nan, A.; Ghandehari, H.; Lee, S. B. Template synthesis of multifunctional nanotubes for controlled release. *J. Controlled Release* **2006**, *114* (2), 143–152.

(29) Geng, Y.; Discher, D. E. Visualization of degradable worm micelle breakdown in relation to drug release. *Polymer* **2006**, *47* (7), 2519–2525.

(30) Cai, S.; Vijayan, K.; Cheng, D.; Lima, E. M.; Discher, D. E. Micelles of different morphologies: advantages of wormlike filomicelles of PEO-PCL in paclitaxel delivery. *Pharm. Res.* **2007**, *24*, 2099–2109.

(31) Geng, Y.; Dalhaimer, P.; Cai, S.; Tsai, R.; Tewari, M.; Minko, T.; Discher, D. E. Shape effects of filaments versus spherical particles in flow and drug delivery. *Nat. Nano* **2007**, *2* (4), 249–255.

BM700888H